Journal of Asian Earth Sciences 166 (2018) 260–269

Contents lists available at ScienceDirect

Journal of Asian Earth Sciences

journal homepage: www.elsevier.com/locate/jseaes

Full length article

Evaluating the state of stress and seismic hazard in Thailand and vicinity through finite element modeling

Beth Meyers[a], Matthew W. Herman[b,*], Kevin P. Furlong[a], Passakorn Pananont[c]

[a] Department of Geosciences, Pennsylvania State University, University Park, PA, USA
[b] Department of Earth Sciences, Utrecht University, Utrecht, Netherlands
[c] Department of Earth Sciences, Kasetsart University, Bangkok, Thailand

ARTICLE INFO

Keywords:
Thailand
Earthquake
Stress field
Finite element modeling

ABSTRACT

Thailand is surrounded by seismically active plate boundary zones and large-offset crustal faults, but there is comparatively little seismic activity within its borders. On 5 May 2014, a moment magnitude (M_W) 6.2 earthquake occurred in the Mae Lao district of northern Thailand. To better anticipate future seismic hazards from events like this, we model the state of stress in Thailand and its vicinity using a finite element approach. We identify northern Thailand as a region with significant stress accumulation, consistent with being caused by convergence at the Sumatra-Andaman subduction zone and southward escape of the Himalayan Orogen. The stress field in this region is compatible with the kinematics of the Mae Lao event. Our modeling also shows that the magnitude of the stress field throughout southeast Asia is particularly sensitive to the stage of the earthquake cycle at the Sumatra-Andaman subduction zone, although the Sumatra-Andaman subduction zone produces a smaller effect on the orientations of stresses in the source region of the Mae Lao earthquake. Finally, we find that the stress change effect from the Mae Lao earthquake is geographically limited and the broader region remains in nearly the same state of stress as prior to the event.

1. Introduction

Most seismically active regions on Earth occur at or near plate boundaries. Although plate interiors lying hundreds of km or more from plate boundaries show low levels of seismic activity, some of these intraplate regions host moderate to large magnitude (moment magnitude Mw 6.0+) earthquakes. This intraplate seismicity often occurs without historic precedent, because earthquakes in such regions commonly have recurrence intervals of many centuries to millennia (Stein, 2007). One model for earthquake genesis in intraplate settings is the reactivation of suitably oriented pre-existing faults or other zones of weakness by stresses built up in the plate interior (Anderson, 1905; Herman et al., 2014). These intraplate stresses can arise from multiple sources (Forsyth and Uyeda, 1975; Wortel et al., 2005; Warners-Ruckstuhl et al., 2013), including interactions with neighboring plates along the plate boundary, gravitational potential energy (GPE) gradients, and tractions at the base of the lithosphere. In particular, the relative motion of adjacent plates past coupled sections of the plate boundary produces significant stress buildup. The stress effects from boundary forces extend through the elastic plates, potentially resulting in seismicity far from high strain-rate plate boundary locations.

A recent example of an intraplate earthquake is the Mw 6.2 event on 5 May 2014 in the Mae Lao District of Thailand, ~27 km southwest of the city of Chiang Rai (hereafter referred to as the "Mae Lao earthquake;" Pananont et al., 2017; Fig. 1). This event is the largest non-subduction-related earthquake ever recorded within Thailand. Despite evidence of active tectonics (high relief and surface evidence for fault structures), the Mae Lao earthquake occurred within an area that historically has had relatively low rates of seismicity. The Mae Lao source region and Thailand more generally sit in a part of southeast Asia that is bounded by zones of substantial lithospheric deformation and higher seismic activity. In this study, we test whether the kinematics of the Mae Lao earthquake are compatible the forces acting along these boundaries of the intraplate region and we use this analysis to identify the potential locations and styles of future seismicity in Thailand and its vicinity.

1.1. Seismo-tectonic setting

The tectonic features surrounding Thailand and its vicinity are largely effects of the north-northeast relative motion of the Indian Plate with respect to the Sunda Block of the Eurasian Plate at a rate of

* Corresponding author.
E-mail address: m.w.herman@uu.nl (M.W. Herman).

https://doi.org/10.1016/j.jseaes.2018.07.030
Received 20 February 2018; Received in revised form 7 June 2018; Accepted 20 July 2018
Available online 01 August 2018

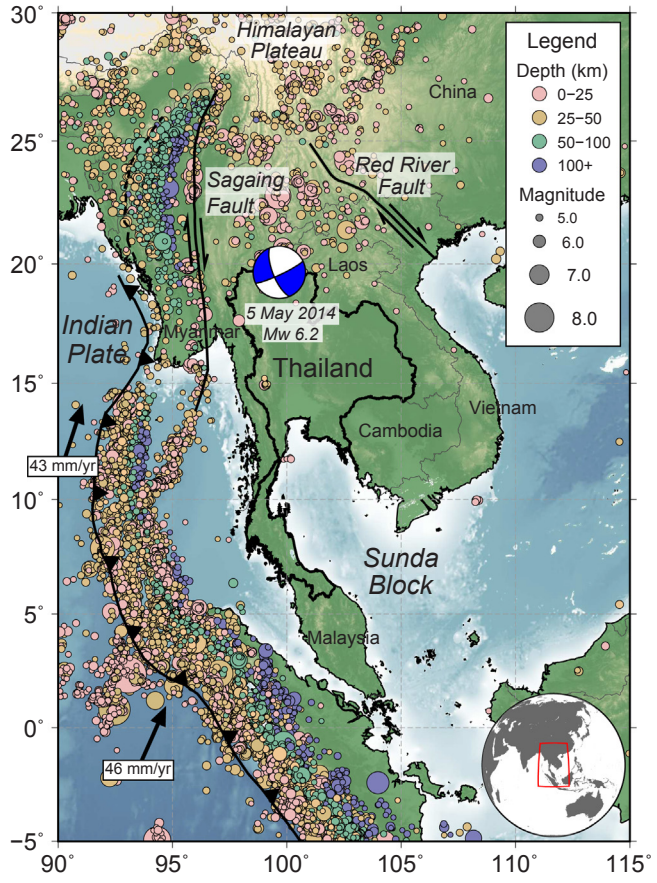

Fig. 1. Tectonic setting of Thailand and vicinity (adapted from Pananont et al., 2017). Plate boundaries and major crustal faults incorporated into the model are plotted as bold black lines. Relative motion vectors between the Indian Plate and the Sunda Block from Argus et al. (2011) are plotted as arrows and labeled with the velocity. Circles indicate historical seismicity with moment magnitude Mw ≥ 4.5 from 1970 to 2017 and are colored by depth and scaled by moment magnitude. The focal mechanism of the 2014 Mw 6.2 Mae Lao earthquake is indicated by the blue beach ball at the event epicenter. (For interpretation of the references to colour in this figure legend, the reader is referred to the web version of this article.)

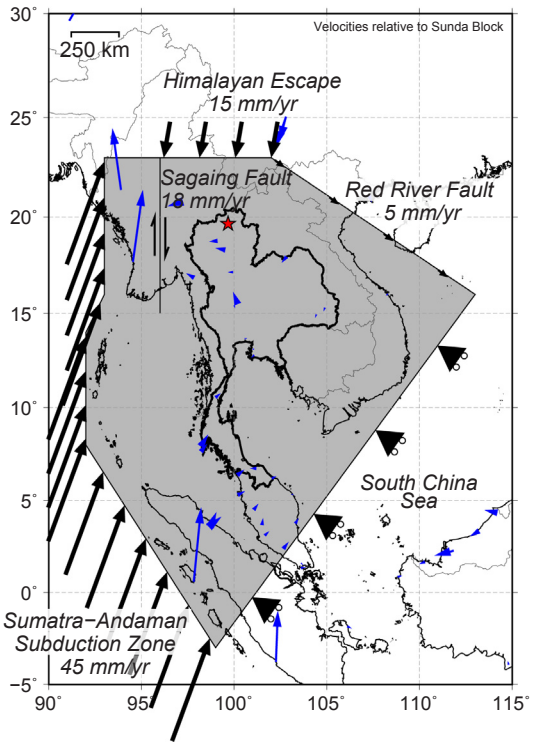

Fig. 2. Model geometry and boundary conditions, plotted on the same map region as in Fig. 1. For reference, the location of the 2014 Mae Lao earthquake is indicated by the red star. Blue arrows represent GPS velocities from Simons et al. (2007) scaled the same as the boundary condition displacements. The northern edge of the model is defined by the southern extent of the Himalayan Orogen, and we apply 15 mm/yr to represent the southward escape tectonics. Along the Red River Fault, we apply 5 mm/yr to the strike-slip feature. At the Sumatra-Andaman subduction zone, we impose 45 mm/yr. We apply 18 mm/yr of right lateral strike-slip motion along the Sagaing Fault. The South China Sea does not move significantly with respect to the Sunda Block, so we fix its motion perpendicular to the boundary, while allowing the boundary to shorten in response to convergence at the Sumatra-Andaman subduction zone.

~45 mm/year (Argus et al., 2011; Fig. 1). There is plate convergence at the Sumatra-Andaman subduction zone west and south of Thailand. Despite several rift basins indicating extension associated with rollback of the subducting slab throughout the Cenozoic, there appears to be little present-day extension in the region (Pubellier and Morley, 2014). The Himalayan Plateau sitting north and west of Thailand extrudes eastward and southward along large-offset strike-slip faults around the edge of the indenting Indian Plate, a process referred to as “escape tectonics” (Tapponnier and Molnar, 1977). Both subduction (including slab rollback) and escape tectonics are inferred to have played an important role in the development of the primary geologic structures in Southeast Asia from the Cenozoic to today (Morley, 2002; Yin, 2010).

Historic seismicity of this region of Southeast Asia is mostly concentrated in the Sumatra-Andaman subduction zone, along the Sagaing Fault through Myanmar, and on strike-slip faults north of Thailand, Laos, and Vietnam (Fig. 1). In Myanmar, west of Thailand, the right-lateral strike-slip Sagaing Fault acts as a continental transform connecting the spreading centers in the Andaman Sea to the continental convergence along the Himalayan front. This structure formed during the early Miocene, and has accommodated 330–450 km of total displacement (Curray, 2005). Slip on the Sagaing Fault accommodates about one third of the plate motion of India relative to the Sunda Block (Simons et al., 2007). This fault hosted three Mw 7–8 earthquakes between 1912 and 1956 (U.S. Geological Survey Comprehensive Catalog; http://earthquake.usgs.gov). In November 2012, a right lateral Mw 6.8 earthquake occurred north of Shwebo, Myanmar, on a northern segment of the Sagaing Fault.

The Red River Fault is a major strike-slip fault northeast of Thailand, and cuts through the Yunnan Province of China and northern Vietnam (northeast of Thailand) as a southern part of the Tibetan fault system (Schoenbohm et al., 2006). This structure is commonly interpreted to be the northeastern limit of the Sunda Block (Simons et al., 2007). Initially left lateral during its formation, the Red River fault has accommodated right lateral motion since the early Pliocene (Zhu et al., 2009). Offsets of Quaternary geomorphic features indicate that the Red River Fault slips in a right lateral sense at a rate of up to 5 mm/year (Trinh et al., 2012), and it has hosted sparse recent seismicity (Fig. 1).

2. Model setup

We estimate the state of lithospheric stress throughout Thailand and its vicinity due to kinematic boundary conditions along the edge of the region using a finite element modeling (FEM) approach. The model is two-dimensional and plane-stress, i.e., it is assumed to be thin in the third (vertical) dimension. Because our goal is to evaluate the effects of boundary conditions on the region of interest, we represent the model domain with a homogeneous elastic material (Young’s modulus = 75 GPa; Poisson’s ratio = 0.30). We do not account for variations in geology, ignoring any associated mechanical

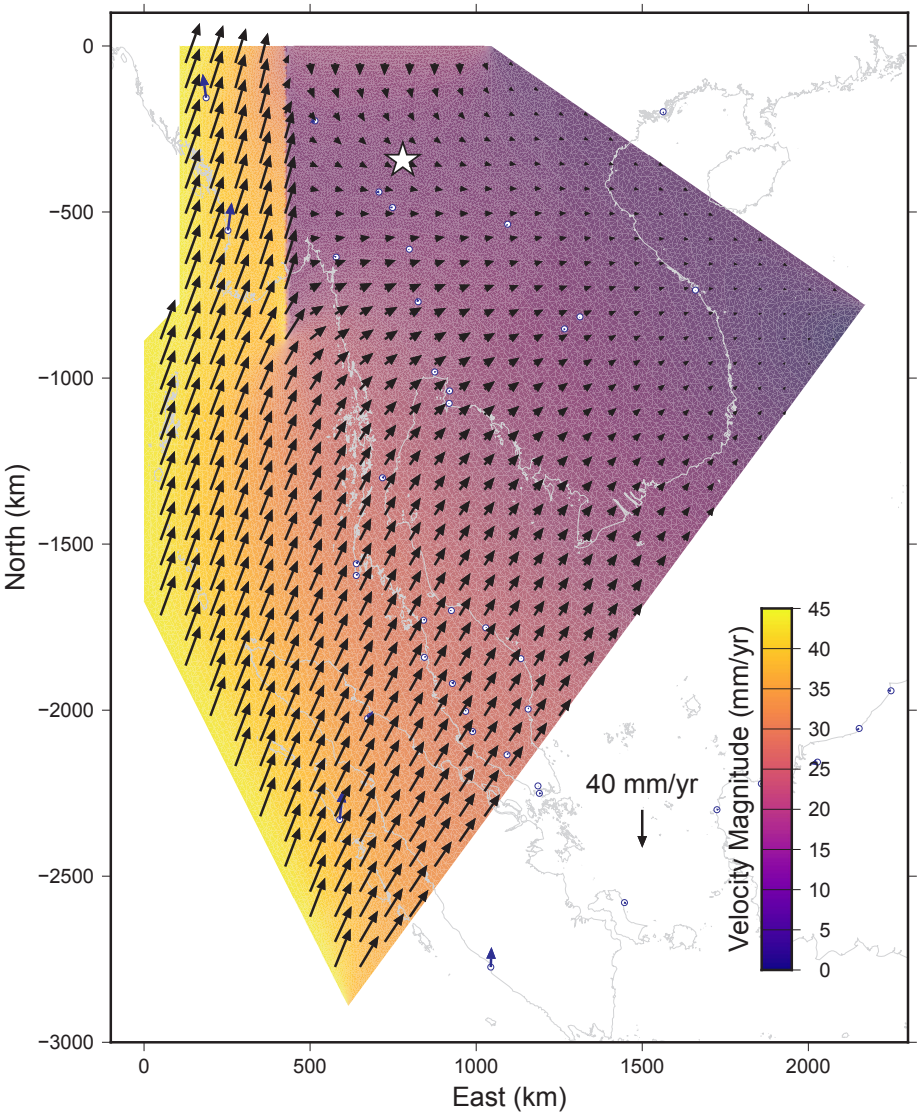

Fig. 3. Velocities produced by our reference model, with coastlines and the 2014 Mae Lao epicenter (white star) shown for reference. Background colors indicate velocity magnitudes. Observed horizontal velocities from Simons et al. (2007) are shown as blue arrows and scaled the same as the model results. (For interpretation of the references to colour in this figure legend, the reader is referred to the web version of this article.)

heterogeneity, rheological complexity, and variations in crustal thickness across the model domain. In particular, we do not model the lateral variations in GPE that also contribute to the stress field (Flesch et al., 2001; Ghosh et al., 2009); the relatively low topographic relief and crustal thickness variations (Noisagool et al., 2014) in Thailand suggest that these GPE-generated stresses will likely be small compared to stresses produced by the boundary forcing. We also ignore mantle tractions, whose contribution to the stress field is not well constrained (Jadamec and Billen, 2010; Warners-Ruckstuhl et al., 2013), and do not consider any ductile deformation.

The model geometry is based on the major faults and plate boundary structures that surround the study area (Fig. 1; Fig. 2). Constraints on the kinematics of plate boundary features come from plate motions, GPS observations, and regional seismicity, which we use to define the precise boundary conditions for the model. The mechanical equilibrium equations for plane stress are solved using the FEM platform GTECTON (version 2011.1.65; Govers and Wortel, 1993) compiled with PETSc 2.3.3 (http://www.mcs.anl.gov/petsc) and the triangular element mesh is refined spatially until the model output does not change with further reduction in element size.

The boundary conditions of the model correspond to the major geologic or tectonic features: the Sumatra-Andaman subduction zone, the Himalayan Orogen, the Red River Fault, the Sagaing Fault, and the South China Sea (Fig. 2). In our reference model, we apply the relative plate velocities or fault slip rates as the boundary conditions to estimate the intraplate loading rate. Because the model is elastic, these results scale linearly with the duration (or displacement) of interest.

The western side of the model domain represents the Sumatra-Andaman subduction zone that lies to the west and southwest of Thailand (Fig. 2). The relative motion between the Indian Plate and Sunda Block along this subduction zone is ~45 mm/yr at an azimuth of ~20° (Argus et al., 2011). Although the India-Sunda relative plate motion is well constrained, subduction zones include a non-horizontal component to their motion at the plate interface due to the descent of the subducting plate. Therefore, the exact horizontal motion to apply along the subduction boundary is uncertain. We use the full plate motion as the velocity boundary condition and recognize that this represents an upper bound on the boundary condition along the subduction zone. We also evaluate how the intraplate stress field depends on the state of the earthquake cycle in the subduction zone; specifically,

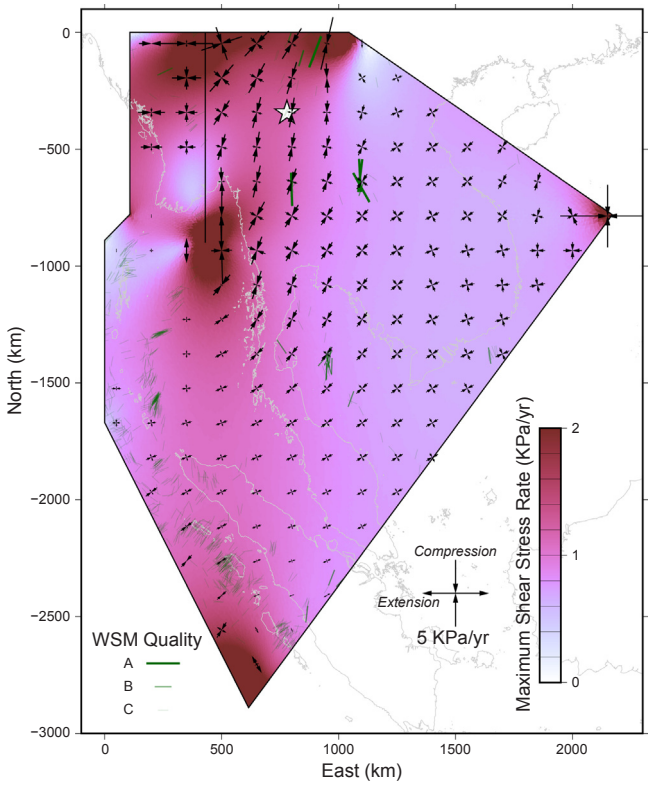

Fig. 4. Principal stressing rate produced by our reference model, with coastlines and the 2014 Mae Lao epicenter (white star) shown for reference. Background colors indicate the maximum shear stressing rate, with darker red colors corresponding to higher values. Arrows indicate the principal stress magnitudes and orientations. Green bars represent Shmax orientations from the World Stress Map Project (Heidbach et al., 2016), with long, bold bars representing high quality data and shorter, lighter bars representing lower quality data. (For interpretation of the references to colour in this figure legend, the reader is referred to the web version of this article.)

we model the effects of the 2004 Mw 9.1 Sumatra-Andaman earthquake. In order to estimate the pre-earthquake stresses, we first integrate the reference model over 500 years (corresponding to a displacement boundary condition along the subduction zone of 22.5 m), which is the approximate recurrence interval of earthquakes on the Sumatra-Andaman subduction plate interface (Rubin et al., 2017). We then compare these results to a model in which the motion along the Sumatra-Andaman boundary is reduced to 5% of the integrated displacement (displacement: 1.13 m), representing near-total co-seismic strain release after the 2004 earthquake (Section 3.3).

The northern boundary of the model represents the forces and displacements associated with tectonic escape of the Himalayan Plateau. In this region, crustal displacements in southern China (relative to a fixed Eurasian Plate) are oriented southward, rotating around the eastern Himalayan syntaxis. This crustal motion occurs at a rate of ~15 mm/yr at an azimuth of 170° (Zhang et al., 2004; Gan et al., 2007). Rotated into the Sunda Block reference frame, these velocities are ~15 mm/yr at 190°. We represent the effects of Himalayan escape tectonics on the Thailand region with these velocity vectors applied as boundary conditions east of the Sagaing Fault at a latitude of 23°N (Fig. 2).

The strike-slip Red River Fault defines the northeastern boundary of the model and is also associated with the tectonic escape of the Himalayan Plateau (Allen et al., 1984). Geodetic observations (Tô et al., 2013) and stream offsets (Schoenbohm et al., 2006) indicate that the Red River Fault currently undergoes right lateral slip at a rate of 2–5 mm/yr, although this slip rate may not be constant with time and may be decreasing (Allen et al., 1984). The effects of the Red River Fault are modeled as a right lateral velocity of 5 mm/yr parallel to the boundary (Fig. 2), which represents an upper bound on the magnitude of the motion that can be generated along this structure. We then examine the sensitivity of the model to reducing this boundary condition magnitude.

Another major crustal fault, the strike-slip Sagaing Fault, extends through and terminates inside of the model domain. Although the Sagaing Fault is curved, in order to simplify its effects, we model the structure as linear (Fig. 2). Geodetic observations indicate that the Sagaing Fault is locked to a depth of ~15 km, and below this depth the slip rate is ~18 mm/yr (Vigny et al., 2003, Maurin et al, 2010). For this locking depth, the two sides of the fault move past each other at the full slip rate at distances greater than ~75 km, which is small compared to the dimensions of our model. Therefore in our reference model, we treat the Sagaing Fault as completely unlocked and sliding at 18 mm/yr. We model the effects of right lateral slip on the Sagaing Fault by using the "split node" formulation (Melosh and Raefsky, 1981), which allows us to introduce kinematically prescribed shear dislocations in the model. We also test the sensitivity of our model to completely locking the Sagaing Fault with no deeper shear zone.

Southeast of Thailand there is no nearby tectonic boundary in the South China Sea, which is an aseismic region containing few significant fault structures. Rather than extend our model domain through the South China Sea beyond our primary region of interest, we draw the southeastern edge of our model in the South China Sea. Geodetic observations near the South China Sea show that this region does not move significantly relative to the Sunda Block, but it does shorten in response to the locked plate interface of the Sumatra-Andaman subduction zone (Iwakuni et al., 2004; Simons et al., 2007). Therefore, we allow this segment to move parallel to the subduction convergence direction while fixing the motion perpendicular to the convergence vector.

3. Results

The FEM allows us to determine the patterns and magnitudes of velocities, strain rate, and stressing rate within the model domain, subject to the applied boundary conditions. In the reference model, the largest velocities are associated with the convergence at the locked subduction zone (Fig. 3). Slip on the Sagaing Fault partitions the velocities in the northern part of the model; the region west of the Sagaing Fault moves northward at 40–45 mm/yr, while the region to the east has velocities lower than 15 mm/yr that are directed southward and eastward. To the south of the Sagaing Fault, there is no internal discontinuity in the model, so velocities change smoothly from 45 mm/yr at the Sumatra-Andaman subduction zone in the southwest to near zero at the Red River Fault in the northeast. Throughout much of mainland Thailand and eastward, predicted velocities are 10 mm/yr or less.

We compare our modeled velocity field to pre-2004 observations from GPS stations in and around Thailand, rotated into the fixed Sunda Block reference frame (Simons et al., 2007) (Fig. 2; Fig. 3). The modeled velocities have comparable magnitudes and orientations to the observed GPS velocities, particularly near the subduction plate boundary and east of the Sagaing Fault. The fit is poorest in the south, where our model has velocities of ~25 mm/yr, whereas the observed velocities are < 5 mm/yr. We note that these misfits are likely results of the simplicity of our model; in addition to the elastic-only assumption, we did not attempt to model the partitioning of slip on other crustal faults (like the Great Sumatran Fault), variations in the mechanical strength of the lithosphere that might affect the intraplate velocity field, or the detailed crustal motions around the boundaries such as those associated with escape tectonics north of Thailand and along the Sagaing and Red River Faults, which are more complex than in our simplified model boundary conditions (Gan et al., 2007).

The pattern of principal stressing rate corresponding to the modeled

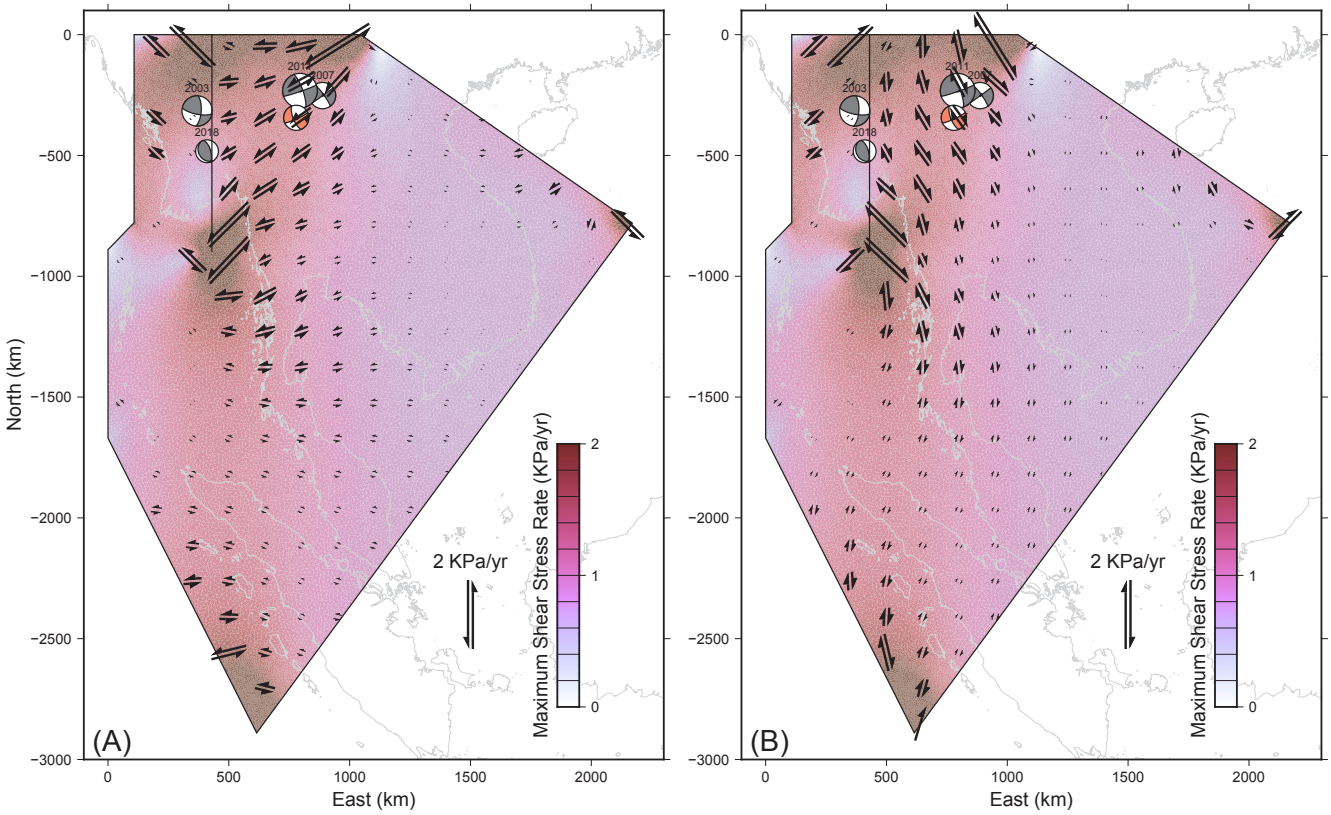

Fig. 5. Maximum horizontal shear stressing rates produced by our reference model, with coastlines, the 2014 Mae Lao focal mechanism (light red), and other Mw 6+ earthquake mechanisms since 2000 (four total events) shown for reference. Background colors indicate maximum shear stress magnitude, as in Fig. 4. (A) Left lateral shear stresses. (B) Right lateral shear stresses. (For interpretation of the references to colour in this figure legend, the reader is referred to the web version of this article.)

velocity field is shown in Fig. 4. Stresses accumulate most rapidly in the model in the northern region, especially between the Sagaing and Red River Faults. The southward directed motion of the Himalayan Plateau along the northern boundary of the model produces dominantly north-south oriented compressional maximum principal stress rates (σ_1) in that area up to 3 KPa/yr. The minimum compressional (or maximum extensional) principal stress (σ_2) throughout this region is compressional and smaller in magnitude than σ_1. Significant extensional stresses are not generated anywhere in the reference model. Farther south, near the Sumatra-Andaman subduction zone, σ_1 is still compressional, relatively smaller in magnitude (~1 KPa/yr), and rotated to NE-SW, subparallel to the subduction convergence direction. Along the Red River Fault boundary and towards the southeastern edge of the model corresponding to the South China Sea, the stresses are compressional and σ_1 and σ_s have similar magnitudes (~2 KPa/yr). The orientations of the principal stress rates generated by the model in central Thailand are compatible with those inferred by Tingay et al. (2010) based on borehole breakouts and earthquake focal mechanisms. Their observations of maximum horizontal stress azimuths (Shmax) are included in the 2016 World Stress Map (Heidbach et al., 2016), which we compare to our model results (Fig. 4). Our model captures many of the regional variations in Shmax azimuth, and although some locations (especially in the southern and central parts of the model) have large angular misfits between modeled and observed Shmax (30° or more), most sites have misfits < 20°.

We also assess the components of stress capable of driving earthquake slip, particularly those that may have been connected to the 2014 Mae Lao earthquake as well as other recent crustal events in the model domain. We found four additional Mw 6+ earthquakes since 2000 from the USGS Comprehensive Catalog for comparison, all of which are in the northern section of the intraplate region (2003 Mw 6.6 in Myanmar; 2007 Mw 6.3 in Laos; 2011 Mw 6.9 in Myanmar; 2018 Mw 6.0 in Myanmar). Maximum horizontal shear stressing rates and azimuths were determined throughout the model (Fig. 5a and b). These are approximately the strike-slip fault orientations with the greatest likelihood of failing in an earthquake, although they do not necessarily coincide with locations and orientations of actual faults. The areas in the model with the largest magnitude shear stressing rates (≥1 KPa/yr) are in the north part of the model, near the Sagaing Fault. It therefore appears to be no coincidence that this area hosted the 2014 Mae Lao earthquake and the other intraplate events since 2000. In addition, the trend in this area with maximum horizontal shear stress is northeast (left-lateral) or southeast (right-lateral), which are similar to the two possible Mae Lao fault plane orientations (Pananont et al., 2017). The other Mw 6+ earthquakes east of the Sagaing Fault have similar focal mechanisms. The 2003 Mw 6.6 event that occurred west of the Sagaing Fault has a strike-slip mechanism rotated ~35° relative to the modeled maximum shear stress azimuth in this region, whereas the 2018 Mw 6.0 thrust faulting earthquake is consistent with the E-W compression west of the Sagaing Fault. These modeled shear stress results indicate that within this intraplate setting, the locations of the Mae Lao and other earthquakes were among those with the greatest chances of failure.

The rate of shear stress accumulation resolved onto left lateral strike-slip faults with a strike of 65° (the kinematics of the Mae Lao earthquake; Pananont et al., 2017) are largest (> 0.5 KPa/yr) east and south of the Sagaing Fault (Fig. 6), Assuming a ~20,000-year recurrence interval, these maximum shear stresses would grow to be > 10 MPa from event to event. For comparison, the Greendale Fault that ruptured in the 2010 Mw 7.0 Darfield, New Zealand, earthquake had a stress drop of 15 MPa (Fry and Gerstenberger, 2011) and was determined to have an average recurrence time of ~25,000 years

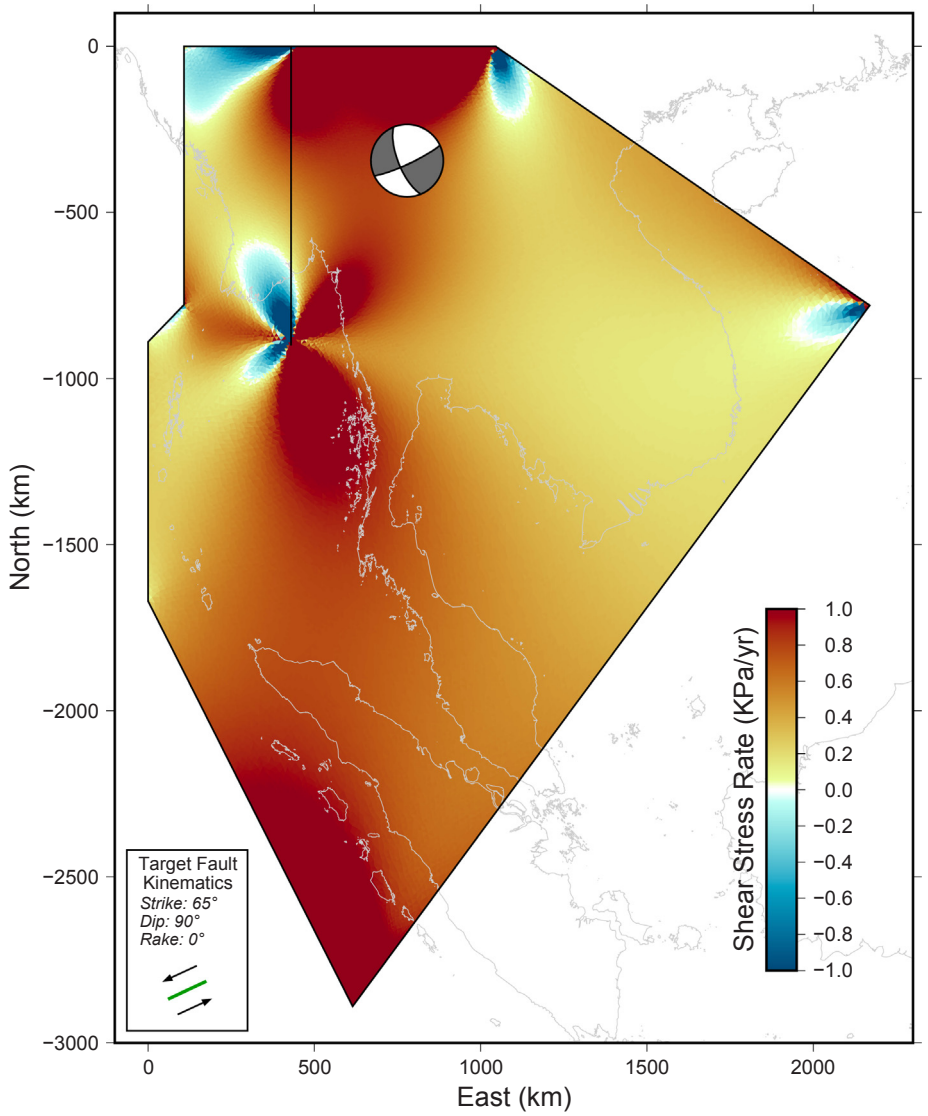

Fig. 6. Shear stressing rate resolved onto the left lateral fault plane of the 2014 Mae Lao event. Note that the shear stress resolved onto the right lateral fault plane is identical. Warm colors indicate areas where slip is promoted and cool colored areas are where slip is inhibited. The Mae Lao earthquake epicenter lies within a region of high shear stress accumulation rate between the Sagaing Fault, the southern extent of the Himalayan Orogen, and the northern Red River Fault.

(Hornblow et al., 2014). These shear stress modeling results indicate that the regional stress fields potentially generated by the boundary conditions acting on the Thailand intraplate region are oriented and distributed in patterns favorable to earthquake activity on faults throughout Thailand.

3.1. Sensitivity to mechanical properties

We test the effects of varying elastic material properties on the resulting displacement and stress fields within the model domain. Because our model is driven by kinematic boundary conditions, the resulting velocity (or displacement) field is entirely insensitive to variations in Young's modulus and has negligible sensitivity to differences in geologically appropriate Poisson's ratios ranging from 0.20 to 0.35. The main consequence of modifying Young's modulus is proportional variations in the subsequent stress values, however the spatial pattern does not change with choice of elastic parameters. Due to the large increase in model parameter space from adding rheological complexity, we do not explore the effects of mechanical heterogeneity, viscous flow, or plastic yielding further in this study.

3.2. Sensitivity to kinematics of escape tectonics

The modeled velocities and stressing rates show little sensitivity to the precise southward kinematics of the Himalayan orogen. We varied the boundary condition magnitude by ± 20% and orientation by ± 20°, corresponding to the variability in observed GPS velocities (Gan et al., 2007). The largest effect is due to variations in the boundary condition magnitude. Decreasing the southward motion of the Himalayan Orogen to 12 mm/yr (increasing to 18 mm/yr) causes the velocities and stresses in northern Thailand to decrease (increase) by a similar factor (Supplementary Figs. 1–16). In none of these sensitivity tests of the escape tectonics do the orientations of motions or stresses change by more than 15°. The highest stressing rates still extend between the Sagaing and Red River Faults and remain compatible with the 2014 Mae Lao earthquake.

Supplementary data associated with this article can be found, in the online version, at https://doi.org/10.1016/j.jseaes.2018.07.030.

3.3. Sensitivity to subduction zone earthquake cycle deformation

Immediately prior to the 2004 Mw 9.1 Sumatra earthquake, it had

been ~500 years since the previous great earthquake (Rubin et al., 2017). Because our model is elastic, the intraplate stresses scale linearly with this duration; therefore, the pattern of stresses is identical to that shown in Figs. 4–6, and the magnitude is simply the rate multiplied by 500 years (Fig. 7a). The 2004 earthquake released much of the elastic strain accumulated at the subduction boundary, which we model by reducing the (now displacement) boundary condition by 95%. This results in a large decrease in the intraplate stresses through the entire model domain (Fig. 7b). The stress field east of the Sagaing Fault continues to be compressed by the southward motion of the Himalayan Plateau in a N-S direction, with principal stress orientations compatible with the kinematics of the 2014 Mae Lao earthquake. The region west of the Sagaing Fault remains in a state of high stress, but closer examination reveals the E-W principal stress has become extensional. In fact, extensional stresses occur throughout the model domain after the 2004 earthquake as a result of co-seismic upper plate extension.

Another major fault structure that may be important to the deformation state in northern Thailand is the Red River Fault. We model a significant earthquake on the Red River fault by reducing the boundary condition displacement here from 5 mm/yr to 0 mm/yr. This has little effect on the velocities or stress rate field throughout the model (Supplementary Figs. 17–20).

Finally, if the Sagaing Fault had a major earthquake that ruptured its entire length, immediately afterwards there would be little remaining unreleased elastic strain along it compared to before the event. Our reference model already incorporates 18 mm/yr of right lateral slip along the Sagaing Fault, effectively simulating the effects of a freely slipping fault, i.e. after an earthquake. If we instead impose no slip on the Sagaing Fault, simulating it as completely locked with no deeper shear zone, the primary difference from the reference model is that velocities and shear stresses are continuous across the Sagaing Fault (Supplementary Figs. 21–24). This increases the shear stresses in the region west of the Sagaing Fault. Otherwise, the magnitudes and orientations of motion and stresses in the model are similar to those in the reference model.

4. Discussion

Our modeling indicates the region where shear stresses accumulate most rapidly (≥1 KPa/yr) in the relatively low-seismicity regions of southeast Asia extends throughout western and northern Thailand, as well as much of Myanmar and northern Laos (Fig. 4). The sensitivity tests demonstrate that the stresses remain high in this region irrespective of the specific stage of the earthquake cycle on major nearby faults, with the exception of the subduction zone. Late in the subduction earthquake cycle (after ~500 years), meters of convergence across the locked fault zone result in a shear stress magnitude in northern Thailand of 0.7 MPa and also produce shear stresses ≥ 0.3 MPa throughout most of Southeast Asia (Fig. 7a). Southeast Vietnam always remains in a relatively low stress state, even late in the subduction earthquake cycle (shear stresses 0.2–0.3 MPa). The subduction earthquake cycle is the dominant process controlling the stress field in Southeast Asia; after an earthquake, shear stress magnitudes are reduced by a factor of ~5 (Fig. 7). At this time, the tectonic escape of the Himalayan Plateau still plays a large role in the stress field in northern Thailand, keeping it in a state of N-S compression. These two boundary processes trade off in dominance depending on the stage of the subduction earthquake cycle, and appear to be locally modulated in the vicinity of northern Thailand by the stage of the earthquake cycle on the Sagaing Fault.

The southward escape tectonics produce north-south oriented maximum (compressional) principal stresses in the northern part of our study region, favoring NE-striking left lateral and SE-striking right lateral earthquakes (Fig. 4). These orientations are compatible with mapped faults in northern Thailand (Thailand Department of Mineral Resources, 2016; Pananont et al., 2017), particularly the SSE-striking right lateral faults and ENE-striking left lateral faults. There is also a population of structures thought to be N-striking normal faults, which we do not analyze in our model, but these faults may be compatible

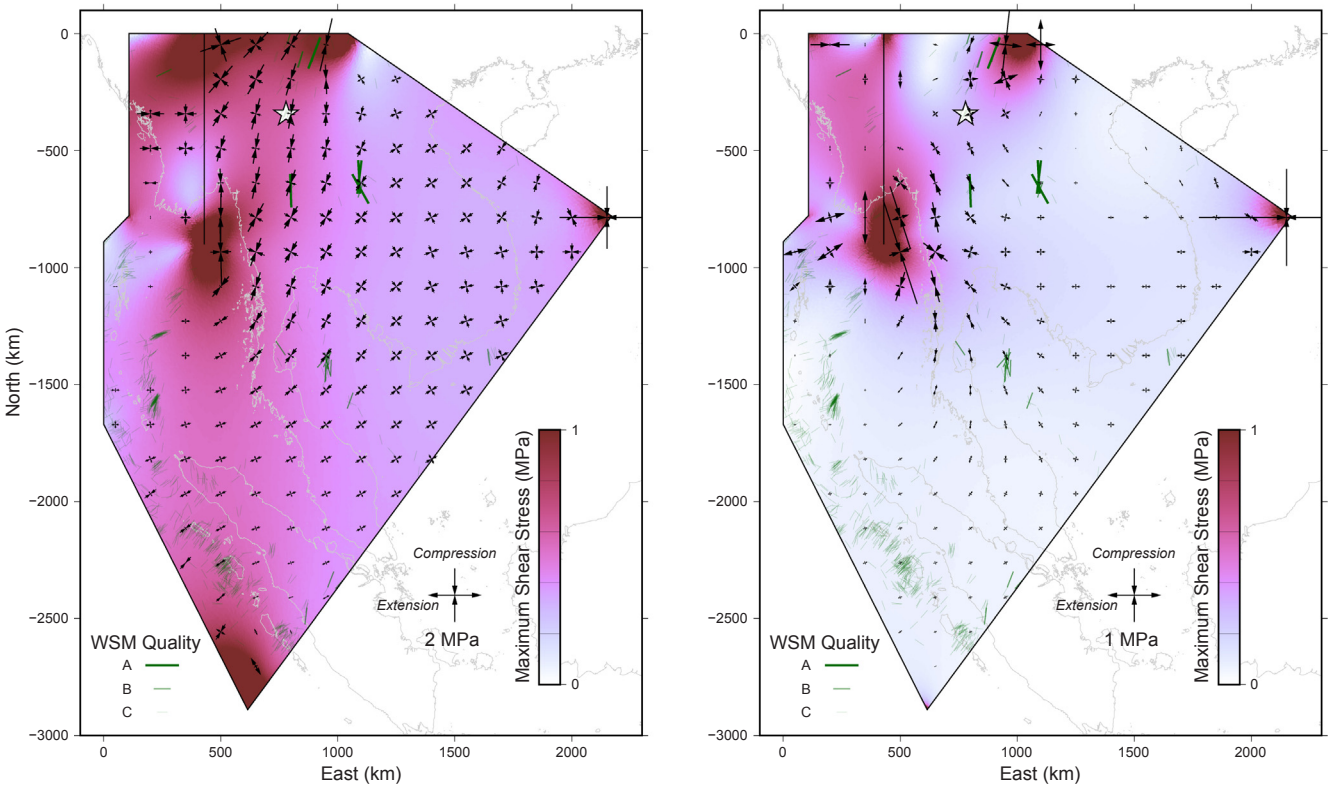

Fig. 7. Time-integrated stresses (A) accumulated in the 500 years before 2004 Mw 9.1 earthquake and (B) after the 2004 earthquake. Color meanings are the same as in Fig. 4, with different scaling. Note that the principal stress arrows have different scales in the two panels.

with slipping soon after a large subduction zone earthquake, when our models show E-W extensional stresses (Fig. 7b). The surface expression of all of these faults suggests that they have been active over the previous few thousand years. Studies of these mapped faults and seismicity Mw ≤ 4.0 were used to identify this region as having a 10% probability of exceeding a peak ground acceleration (PGA) of 0.15 g for a 50-year time window (Ornthammarath et al., 2011).

4.1. 2014 Mae Lao earthquake

On 5 May 2014, the Mw 6.2 Mae Lao earthquake occurred in this region of mapped faults, within an area inferred to have high fluid content (Boonchaisuk et al., 2017). The event produced a maximum PGA of 0.30 g measured on top of a dam 15 km from the epicenter and 0.13 g at a ground-based station 27 km from the epicenter (Ornthammarath and Warnitchai, 2015), consistent with the previously estimated hazard probabilities. The event had a strike-slip mechanism (Noisagool et al., 2016: strike = 260°, dip = 90°, rake = −5°; Pananont et al., 2017: strike = 163°, dip = 80°, rake = 169°). Pananont et al. (2017) also showed how this earthquake and its aftershock sequence ruptured two conjugate strike-slip faults, both of which are compatible with a NNE-trending direction of maximum compression.

A key question following this event is how it perturbed the regional stress field and the implications for future seismic hazards. We evaluate post-Mae Lao earthquake stresses by computing the co-seismic stress change and adding that to the modeled 500-year regional stress field. We assume that the earthquake occurred at 10 km depth in an elastic half-space with the same material properties as the FEM, then use the equations of Okada (1992) to compute the co-seismic stress change at the same depth as the earthquake. We add the resulting co-seismic stresses to the FEM stress field and compute the shear stresses resolved on faults with the same geometry as the Mae Lao earthquake (Fig. 8). Because the event is small compared to the spatial scale of the region, it acts like a point source and is therefore insensitive to our choice of fault plane or empirical relation to determine the rupture size (Supplementary Fig. 25). The earthquake reduced regional stresses over a ~50 km long region, consistent with the dimensions of the stress footprint discussed in Pananont et al. (2017). The pre-2014 level of shear stress at the location of the earthquake and resolved onto the fault geometry in our 500-year model is ~3 MPa. Therefore, we estimate that the event, which had a stress drop of ~4 MPa (Ornthammarath and Warnitchai, 2015), released 700–800 years of stress accumulation over a 50-km-

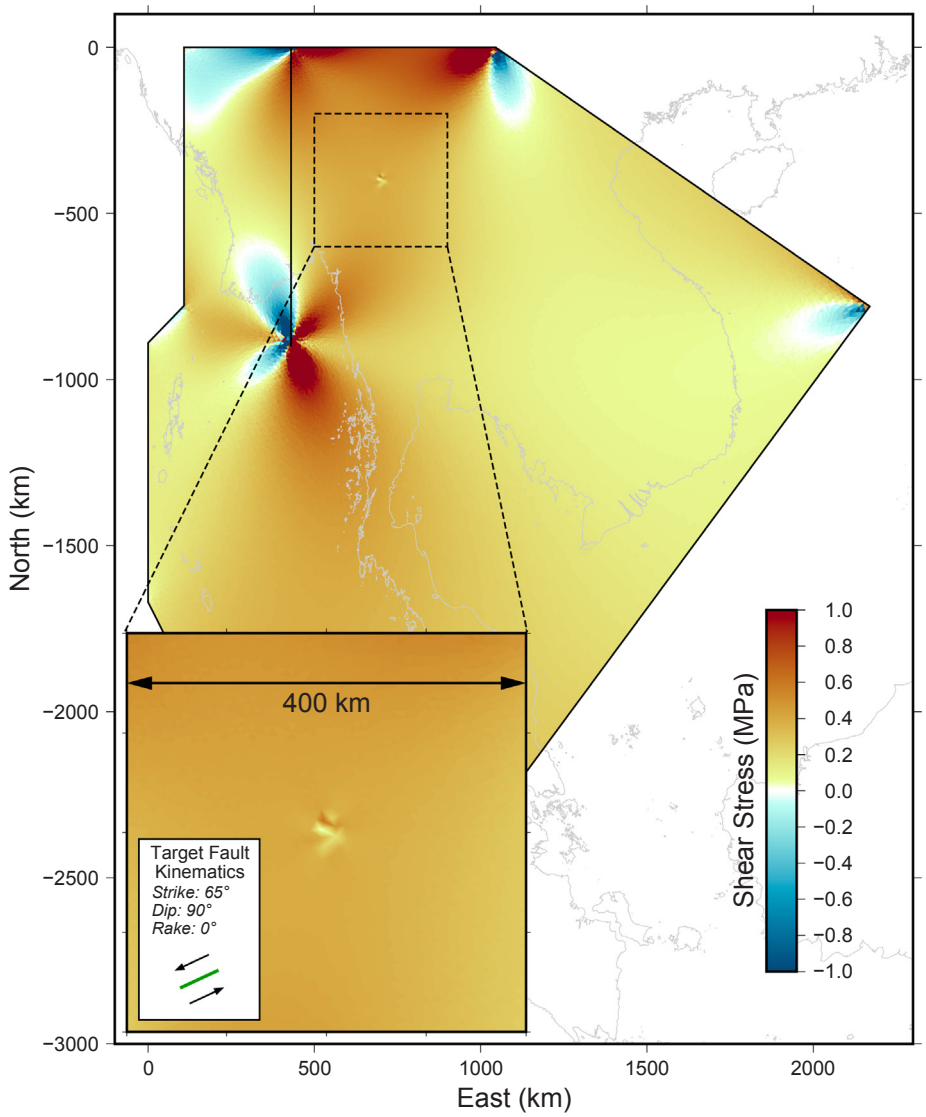

Fig. 8. 500-year shear stresses resolved onto the left lateral fault plane of the 2014 Mae Lao earthquake, plus the co-seismic stress changes of the Mae Lao earthquake (assuming the left lateral fault plane: strike = 255°, dip = 80°, rake = 10°). Inset figure shows the sum of these stress fields in a 400-km wide region around the earthquake epicenter. This earthquake did little to perturb the stress field outside of a ~50 km diameter region surrounding the epicenter.

wide region. However, the greater northern Thailand region is essentially unaffected by the Mae Lao earthquake, and still remains in essentially the same state of stress that drove the 2014 event.

The small effect of the 2014 Mae Lao earthquake on the intraplate stress field is consistent with interpretations from other similar regions. For example, the Canterbury Plains in South Island, New Zealand, experienced a sequence of Mw 6.0–7.0 earthquakes from 2010 to 2011. Herman et al. (2014) showed that these events caused negligible perturbations to the regional stress field as measured by aftershock P-axis orientations, except perhaps near the ends of the rupture zones of the largest events. In addition, they showed that the broader Canterbury Plains remains in a state of stress favorable for slip on a similarly oriented structure. Thailand and its vicinity can be interpreted in a similar way. Although the seismic hazard on the fault that hosted the Mae Lao earthquake and its aftershock sequence are now likely reduced, the event may have brought nearby structures closer to failure, and the broader Thailand region should be considered to have a similar seismic hazard as prior to the Mae Lao earthquake.

5. Conclusion

The stress field throughout much of Southeast Asia is consistent with being produced primarily by interactions with adjacent plates along four major boundaries: the Himalayan Orogen, the Sumatra-Andaman subduction zone, the Red River Fault, and the Sagaing Fault. The coupling state of the subduction zone plays a dominant role in the stresses throughout the intraplate region. The southward escape of the Himalayan Plateau controls the orientation of the stress field in the vicinity of northern Thailand, favoring NE-striking left lateral and SE-striking right lateral strike-slip faulting, as in the 2014 Mw 6.2 Mae Lao earthquake. This earthquake locally modified the stress field, but the regional state of stress (and the corresponding seismic hazard) remains essentially the same throughout northern Thailand after this earthquake.

Acknowledgements

We thank R. Govers for providing useful feedback on the manuscript. Many of the figures were produced using GMT (Wessel and Smith, 1991). Two anonymous reviewers provided helpful feedback that improved the manuscript. M.W. Herman was funded by NASA Earth and Space Science Fellowship #NNX14AL21H. P. Pananont was funded by Thailand Research Fund Grant # RDG6030017.

References

Allen, C.R., Gillespie, A.R., Yuan, H., Sieh, K.E., Buchun, Z., Chengnan, Z., 1984. Red River and associated faults, Yunnan Province, China: Quaternary geology, slip rates, and seismic hazard. Geol. Soc. Am. Bull. 95, 686–700. https://doi.org/10.1130/0016-7606(1984) 95<686:RRAAFY>2.0.CO;2.

Anderson, E.M., 1905. The dynamics of faulting. Trans. Edinburgh Geol. Soc. 8, 387–402.

Argus, D.F., Gordon, R.G., DeMets, C., 2011. Geologically current motion of 56 plates relative to the no-net-rotation reference frame. Geochem. Geophys. Geosyst. 12, 1–13. https://doi.org/10.1029/2011GC003751.

Boonchaisuk, S., Noisagool, S., Amatyakul, P., Rung-Arunwan, T., Vachiratienchai, C., Siripunvaraporn, W., 2017. 3-D magnetotelluric imaging of the Phayao Fault Zone, Northern Thailand: Evidence for saline fluid in the source region of the 2014 Chiang Rai earthquake. J. Asian Earth Sci. 147, 210–221. https://doi.org/10.1016/j.jseaes.2017.07.034.

Curray, J.R., 2005. Tectonics and history of the Andaman Sea region. J. Asian Earth Sci. 25, 187–232. https://doi.org/10.1016/j.jseaes.2004.09.001.

Flesch, L.M., Haines, A.J., Holt, W.E., 2001. Dynamics of the India-Eurasia collision zone. J. Geophys. Res. 106 (B8), 16435–16460.

Forsyth, D., Uyeda, S., 1975. On the relative importance of the driving forces of plate motion. Geophys. J. R. Astron. Soc. 43, 163–200. https://doi.org/10.1111/j.1365-246X.1975.tb00631.x.

Fry, B., Gerstenberger, M.C., 2011. Large apparent stresses from the Canterbury earthquakes of 2010 and 2011. Seismol. Res. Lett. 82, 833–838. https://doi.org/10.1785/gssrl.82.6.833.

Gan, W., Zhang, P., Shen, Z.-K., Niu, Z., Wang, M., Wan, Y., Zhou, D., Cheng, J., 2007. Present-day crustal motion within the Tibetan Plateau inferred from GPS measurements. J. Geophys. Res. 112, B08416. https://doi.org/10.1029/2005JB004120.

Ghosh, A., Holt, W.E., Flesch, L.M., 2009. Contribution of gravitational potential energy differences to the global stress field. Geophys. J. Int. 179 (2), 787–812. https://doi.org/10.1111/j.1365-246X.2009.04326.x.

Govers, R., Wortel, M.J.R., 1993. Initiation of asymmetric extension in continental lithosphere. Tectonophysics 223, 75–96. https://doi.org/10.1016/0040-1951(93)90159-H.

Heidbach, O., Rajabi, M., Reiter, K., Ziegler, M., Team, W.S.M., 2016. World stress map database release 2016. GFZ Data Services. https://doi.org/10.5880/WSM.2016.001.

Herman, M.W., Herrmann, R.B., Benz, H.M., Furlong, K.P., 2014. Using regional moment tensors to constrain the kinematics and stress evolution of the 2010–2013 Canterbury earthquake sequence, South Island, New Zealand. Tectonophysics 633, 1–15. https://doi.org/10.1016/j.tecto.2014.06.019.

Hornblow, S., Quigley, M., Nicol, A., Van Dissen, R., Wang, N., 2014. Paleoseismology of the 2010 Mw 7.1 Darfield (Canterbury) earthquake source, Greendale Fault, New Zealand. Tectonophysics 637, 178–190. https://doi.org/10.1016/j.tecto.2014.10.004.

Iwakuni, M., Kato, T., Takiguchi, H., Nakaegawa, T., Satomura, M., 2004. Crustal deformation in Thailand and tectonics of Indochina peninsula as seen from GPS observations. Geophys. Res. Lett. 31 (11). https://doi.org/10.1029/2004GL020347. n/a–n/a.

Jadamec, M.A., Billen, M.I., 2010. Reconciling surface plate motions with rapid three-dimensional mantle flow around a slab edge. Nature 465 (7296), 338–341. https://doi.org/10.1038/nature09053.

Maurin, T., Masson, F., Rangin, C., Min, U.T., Collard, P., 2010. First global positioning system results in northern Myanmar: Constant and localized slip rate along the Sagaing fault. Geology 38, 591–594. https://doi.org/10.1130/G30872.1.

Melosh, H.J., Raefsky, A., 1981. A simple and efficient method for introducing faults into finite element computations. Bull. Seismol. Soc. Am. 71, 1391–1400.

Morley, C.K., 2002. A tectonic model for the Tertiary evolution of strike-slip faults and rift basins in SE Asia. Tectonophysics 347, 189–215. https://doi.org/10.1016/S0040-1951(02)00061-6.

Noisagool, S., Boonchaisuk, S., Pornsopin, P., Siripunvaraporn, W., 2014. Thailand's crustal properties from tele-seismic receiver function studies. Tectonophysics 632 (C), 64–75. https://doi.org/10.1016/j.tecto.2014.06.014.

Noisagool, S., Boonchaisuk, S., Pornsopin, P., Siripunvaraporn, W., 2016. The regional moment tensor of the 5 May 2014 Chiang Rai earthquake (Mw = 6.5), Northern Thailand, with its aftershocks and its implication to the stress and the instability of the Phayao Fault Zone. J. Asian Earth Sci. 127, 231–245. https://doi.org/10.1016/j.jseaes.2016.06.008.

Okada, Y., 1992. Internal deformation due to shear and tensile faults in a half-space. Bull. Seismol. Soc. Am. 82, 1018–1040.

Ornthammarath, T., Warnitchai, P., Worakanchana, K., Zaman, S., Sigbjörnsson, R., Lai, C.G., 2011. Probabilistic seismic hazard assessment for Thailand. Bull. Earthq. Eng. 9, 367–394. https://doi.org/10.1007/s10518-010-9197-3.

Ornthammarath, T., Warnitchai, P., 2015. The 5 May 2014 MW 6.1 Mae Lao (Northern Thailand) earthquake: Interpretations of recorded ground motion and structural damage. Earthquake Spectra.

Pananont, P., Herman, M.W., Pornsopin, P., Furlong, K.P., Habangkaem, S., Waldhauser, F., Wongwai, W., Limpisawad, S., Warnitchai, P., Kosuwan, S., Wechbunthung, B., 2017. Seismotectonics of the 2014 Chiang Rai, Thailand, earthquake sequence. J. Geophys. Res. 122, 6367–6388. https://doi.org/10.1002/2017JB014085.

Pubellier, M., Morley, C.K., 2014. The basins of Sundaland (SE Asia): Evolution and boundary conditions. Mar. Pet. Geol. 58, 555–578. https://doi.org/10.1016/j.marpetgeo.2013.11.019.

Rubin, C.M., Horton, B.P., Sieh, K., Pilarczyk, J.E., Daly, P., Ismail, N., Parnell, A.C., 2017. Highly variable recurrence of tsunamis in the 7,400 years before the 2004 Indian Ocean tsunami. Nat. Commun. 8, 16019. https://doi.org/10.1038/ncomms16019.

Schoenbohm, L.M., Burchfiel, B.C., Liangzhong, C., Jiyun, Y., 2006. Miocene to present activity along the Red River fault, China, in the context of continental extrusion, upper-crustal rotation, and lower-crustal flow. Geol. Soc. Am. Bull. 118, 672–688. https://doi.org/10.1130/B25816.1.

Simons, W.J.F., Socquet, A., Vigny, C., Ambrosius, B.A.C., Haji Abu, S., Promthong, C., Subarya, C., Sarsito, D., Matheussen, S., Morgan, P., Spakman, W., 2007. A decade of GPS in Southeast Asia: Resolving Sundaland motion and boundaries. J. Geophys. Res. 112, B06420. https://doi.org/10.1029/2005JB003868.

Stein, S., 2007. Approaches to continental intraplate earthquake issues. In: Continental Intraplate Earthquakes: Science, Hazard, and Policy Issues. Geological Society of America, pp. 1–16. https://doi.org/10.1130/2007.2425(01).

Tapponnier, P., Molnar, P., 1977. Active faulting and tectonics in China. J. Geophys. Res. 82, 2905–2930. https://doi.org/10.1029/JB082i020p02905.

Thailand Department of Mineral Resources, 2016. Active fault map of Thailand.

Tingay, M., Morley, C., King, R., Hillis, R., Coblentz, D., Hall, R., 2010. Present-day stress field of Southeast Asia. Tectonophysics 482, 92–104. https://doi.org/10.1016/j.tecto.2009.06.019.

Tô, T.Đ., Yêm, N.T., Công, D.C., Hải, V.Q., Zuchiewicz, W., Cu'ò'ng, N.Q., Nghĩa, N.V., 2013. Recent crustal movements of northern Vietnam from GPS data. J. Geodyn. 69, 5–10. https://doi.org/10.1016/j.jog.2012.02.009.

Trinh, P.T., Van Liem, N., Van Huong, N., Vinh, H.Q., Van Thom, B., Thao, B.T., et al., 2012. Late Quaternary tectonics and seismotectonics along the Red River fault zone, North Vietnam. Earth Sci. Rev. 114, 224–235. https://doi.org/10.1016/j.earscirev.2012.06.008.

Vigny, C., Socquet, A., Rangin, C., Chamot-Rooke, N., Pubellier, M., Bouin, M., Bertrand, G., Becker, M., 2003. Present-day crustal deformation around Sagaing fault, Myanmar. J. Geophys. Res. 108, 2533. https://doi.org/10.1029/2002JB001999.

Warners-Ruckstuhl, K.N., Govers, R., Wortel, R., 2013. Tethyan collision forces and the stress field of the Eurasian Plate. Geophys. J. Int. 195 (1), 1–15. https://doi.org/10.1093/gji/ggt219.
Wessel, P., Smith, W.H.F., 1991. Free software helps map and display data. Eos 72, 441–446.
Wortel, M.J.R., Remkes, M.J.N., Govers, R., Cloetingh, S.A.P.L., Meijer, P.T., 2005. Dynamics of the lithosphere and the intraplate stress field. Philos. Trans. Royal Soc. London. Ser. A 337, 111–126.
Yin, A., 2010. Cenozoic tectonic evolution of Asia: A preliminary synthesis. Tectonophysics 488, 293–325. https://doi.org/10.1016/j.tecto.2009.06.002.
Zhang, P.-Z., Shen, Z., Wang, M., Gan, W., Bürgmann, R., Molnar, P., Wang, Q., Niu, Z., Sun, J., Wu, J., Hanrong, S., Xinzhao, Y., 2004. Continuous deformation of the Tibetan Plateau from global positioning system data. Geology 32, 809. https://doi.org/10.1130/G20554.1.
Zhu, M., Graham, S., McHargue, T., 2009. The red river fault zone in the Yinggehai Basin, South China Sea. Tectonophysics 476, 397–417. https://doi.org/10.1016/j.tecto.2009.06.015.